Congresso de Métodos Numéricos em Engenharia 2015
Lisboa, 29 de Junho a 2 de Julho 2015

THE COMPUTATION DYNAMICS OF ELECTROMAGNETIC RADIATION IN 3D DISPERSIVE METAMATERIALS.

Erika Martínez-Sánchez[1] and Gennadiy Burlak[1*]

1: Centro de Investigación en Ingeniería y Ciencias Aplicadas
Universidad Autónoma del Estado de Morelos, 62209
erika.martinez@uaem.mx, gburlak@uaem.mx

Keywords: Numerical simulation, Numerical Methods, 3D Dispersive metamaterial, FDTD, Photonic crystals, Parallel calculations

Abstract. *We numerically investigated the complex dynamics of the electromagnetic radiation generated by the charged particles crossing 3D dispersive nano metamaterials. In our theory only parameters of a medium are fixed, while the frequency spectrum of the internal excitations is left to be defined as a result of numerical calculations. Accurate numerical simulations (with the use of 3D Drude model) show that the periodic field structure coupled to plasmonic excitations is arisen when the dispersive refractive index of such a system becomes negative. In this case the reversed Cherenkov radiation can be observed. The specific resonant field interferences in the frequency range with the negative refractive index of a metamaterial is registered. The results of numerical simulations show that the frequency spectra (resonances) of the plasmonic excitations are formed due to the nonlinear fields interplay in the frequency domain. The application of photonic crystals and the parallel schemes for numerical simulations in such a coupled problem is also discussed.*

1 INTRODUCTION

Nanophotonics is the study of the behavior of light on the nanometer scale with involving the interaction of light with nano-structures. Novel optical properties of materials results from their extremely small size that have a variety of applications in nanophotonics and plasmonics. The investigations of optical negative-index [1] metamaterials (NIM) using the nanostructured metal–dielectric composites already have led to both fundamental and applied achievements that have been realized in various structures [2]–[24]. The main applications of negative index metamaterials (or left-handed materials (LHM)) are connected with a remarkable property: the direction of the energy flow and the direction of the phase velocity are opposite in NIM that results unusual properties of electromagnetic waves propagating in these mediums.

Cherenkov radiation by a charged source that moves in a left-handed material and has not the own frequency has been studied in number of works [17]–[24]. Both experimental

and theoretical frameworks are investigated, see review [18] and references therein. However in some important cases a moving particle has the internal own frequency[25] ω_0, for instance the ion oscillating at the transition frequency ω_0. The Cherenkov emission in metamaterials for such situation is insufficiently investigated yet, although it is a logical extension of other works in this area.

In this paper the Cherenkov optical radiation in 3D metamaterials by a nonrelativistic modulated source having the own frequency ω_0 with an emphasis on the dispersive properties of the medium is numerically studied. We performed the FDTD simulations with the use of the material parameters at various modulating frequencies ω_0, however without references to the operational frequency range.

2 BASIC EQUATIONS

In metamaterials, it is necessary to treat electromagnetic wave interactions with a metal ingredient using a dispersive formulation that allows correct description of the internal electron dynamics. In this paper we exploit the Drude model that became widely used for modeling in complex materials where for a range of frequency the negative refraction index n is expected. The Maxwell equations read

$$\nabla \times \mathbf{E} = -\mu_0 \mu_h \frac{\partial \mathbf{H}}{\partial t} - \mathbf{J}_m - \sigma_m \mathbf{H}, \tag{1}$$

$$\nabla \times \mathbf{H} = \varepsilon_0 \varepsilon_h \frac{\partial \mathbf{E}}{\partial t} + q\mathbf{v}_0 f(r,t)\cos(\omega_0 t) + \mathbf{J}_e + \sigma_e \mathbf{E}, \tag{2}$$

where a radiating particle (bunch) has modulating frequency ω_0, $\mathbf{J}_e$ is the electrical current and $\mathbf{J}_m$ is the magnetic current which obey the following material equations

$$\dot{\mathbf{J}}_e + \gamma_e \mathbf{J}_e = b_e \mathbf{E}, \quad \dot{\mathbf{J}}_m + \gamma_m \mathbf{J}_m = b_m \mathbf{H}, \tag{3}$$

here γ_e and γ_m are the electrical and magnetic collision frequencies respectively, $b_e = \varepsilon_0 \omega_{pe}^2$, $b_m = \mu_0 \omega_{pm}^2$, ω_{pe} and ω_{pm} are frequencies of electric and magnetic plasmons respectively, σ_e and σ_m are conductivities, ε_h, μ_h are dielectric and magnetic functions of the host medium respectively [26], [27]. For metals such as silver, gold, copper and aluminum the density of the free electrons is on the order of $10^{23} cm^{-3}$. The typical value $\omega_{pe} \approx 2 \cdot 10^{16} s^{-1}$ ([28], p.44). In a metamaterial with fishnet structure [14] we consider the charge particle (charge q) moving with a uniform velocity parallel to x direction: $\mathbf{v}_0 \parallel \widehat{\mathbf{e}}_x$ and the density of the particle is defined by the Gaussian as $f(r,t) = W^{-3} \exp\{-[(x - v_0 t)^2 + y^2 + z^2]/W^2\}$, where W is the width; at $W \to 0$ such a distribution is simplified to the isotropic point-source distribution $f(r,t) \to (\pi)^{3/2} \delta(x - v_0 t)\delta(y)\delta(z)$. In the following for simulations we use dimensionless variables, where for renormalization are used: the vacuum light velocity $c = (\varepsilon_0 \mu_0)^{-0.5}$ and the typical spatial scale for nanooptics objects $l_0 = 75nm$. With such a normalization above indicated the metal plasma frequency becomes $\omega_{pe} = 5$. The electrical and magnetic fields are renormalized with the electrical scale $E_0 =$

$ql_0\varepsilon_0$ and magnetic scale $H_0 = (\varepsilon_0/\mu_0)^{0.5}E_0$ respectively. Some metamaterials exhibit anisotropic properties with tensor permittivity and permeability. To seek for simplicity in this paper we concentrated in the isotropic geometry. Modeling anisotropic medium is a straightforward extension of this model, see details in Refs. [18], [24].

In our FDTD simulations (in time domain) we use the following idea. In optical experiments normally one refers only to the parameters of material (γ_e, σ_e, ω_{pe}, and γ_m, σ_m, ω_{pm}). Therefore we consider the Cherenkov emission produced by a particle with modulating frequency ω_0, with the use only the material parameters and without of references to the operational frequency band. In this approach the frequency spectrum of internal excitations ω is left as a free parameter that is defined from simulations by a self-consistent way. For 3D dispersion material such a problem becomes too difficult for analytical consideration. In this paper the well-known numerical algorithms in the time domain[29] were used, for details see Ref.[11].

General 3D case in Cartesian coordinates is considered since such a geometry normally is used on the optical investigations [14]. We examine a spatially averaged metamaterial composition: nanostructured metal–dielectric composites (fishnet), similarly that was used in the experiment [14]. In this case the spatial average scale is less then the infrared and visual wavelengths, so we can deem that the material (dielectric and magnetic) dispersion is allowed by the Drude model and the role of the active dielectric ingredient is reduced to a compensation of losses due to the metal ingredient. In our simulations was used the numerical grid L^3, $L = 100,120,150$, for more details see Ref.[11].

The following steps have been used in our approach: (i) First, we calculated the time-spatial field dynamics that is raised by the crossing radiating particle for different modulating frequencies ω_0, Eqs.(1)-(3). (ii) In second step we applied the Fourier analysis for the time and spatial dependencies of the field calculated in the first step in order to reveal the dynamics and spectrum of internal excitations. The following dimensionless parameters were used in our simulations: $\omega_{pe} = 5$, $\omega_{pm} = 7$, $\varepsilon_h = 1.44$, $\mu_h = 1$, $\gamma_e = \gamma_m = 10^{-4}$, $\sigma_e = \sigma_m = 10^{-7}$, $W = 4$, $q_2 = 2$. We also varied the particle velocity v_0 for different ω_0 to study regimes of the Cherenkov emission. Our results are shown in Figs (1)-(5).

Fig.1 shows the spatial structure of $E_x(r,t)$ field for the particle with modulating frequency ω_0 that moves with uniform velocity $v_0 = 0.52$. Fig.1 (a) depicts the case $\omega_0 = 0$; in this situation only the spectrum of the periodic plasmonic excitations with the frequency ω_C and negative phase velocity is observed (see details in Ref.[11]). At the increase of ω_0 up to 6 (see Fig.1 (b), (c) and (d) respectively) the spatial field structure changes considerably. For $\omega_0 = 2$ and $\omega_0 = 6$ (see Fig.1 (b) and (d) respectively) the field has oscillating shape, but for $\omega_0 = 4$ in Fig.1 (c) the field acquires a near monotonic form.

In what follows we use the complementary Cherenkov emission angle $\theta_1 = \pi/2 - \theta$, where [26] $\cos(\theta) = c/nv_0$. For such angle we have[11] $\cos(\theta) = \sin(\theta_1) = c/nv_0$, so for conventional material (with $Re(n) > 0$) θ_1 is positive $\theta_1 = \theta_{1+} > 0$, while for negative refraction index metamaterial NIM (with $Re(n) < 0$) θ_1 is negative $\theta_1 = \theta_{1-} < 0$. From

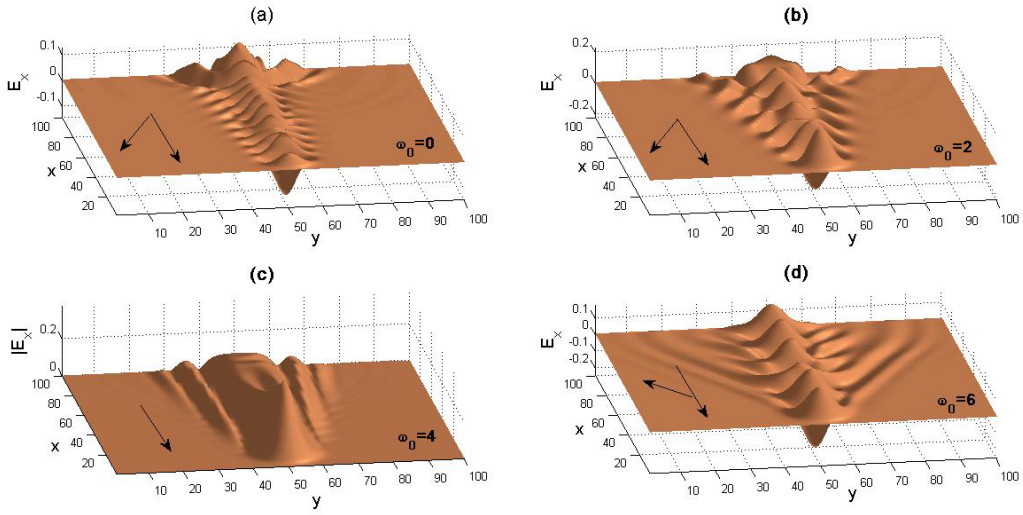

Figure 1: Snapshots of the Cherenkov field emission $E_x(\mathbf{r},t)$ generated by radiating particle with velocity $v_0 = 0.52$ for different frequencies ω_0 at time $t \simeq 190$ in a dispersive metamaterial. (a) $\omega_0 = 0$, in this case the complementary Cherenkov angle is negative $\theta_1 < 0$; (b) $\omega_0 = 2.0$, $\theta_1 < 0$; (c) $\omega_0 = 4.0$, $\theta_1 \simeq 0$; (d) $\omega_0 = 6.0$, in this case the angle is positive $\theta_1 > 0$. The oscillations in the top of the figures exhibit the shock waves arising by charged source at the beginning of motion. See details in text.

Fig.1 we observe that for frequencies $\omega_0 \leq 3$ the angle θ_1 is negative what corresponds to the reverse Cherenkov radiation. But for larger $\omega_0 \geq 6$ the Cherenkov radiation already acquires conventional structure with positive $\theta_1 > 0$, see Fig.1 (d). More interesting is found the intermediate case with $\omega_0 \simeq 4$ where the field acquires nearly monotonic shape, see Fig.1 (c). Such a behavior can be interpreted as a transition in the spectra of plasmonic-polariton excitations. Further we study such field behavior with details.

The interesting question emerges, why the structure of field in Fig.1 changes so considerably with the change of the modulating frequency ω_0? To study that we explore the variation of the field spatial structure in the wavenumber domain (k) at the change ω_0. It is instructively to compare the field spatial structure with $\omega_0 = 0$ in NIM with other modulated particle case when $\omega_0 \neq 0$ but in a *dispersiveless* material (with $\omega_{pe} = \omega_{pm} = 0$). (Such an evaluation in principle could be done similarly to the *Liènard-Wiechert potentials* approach[26], but analytical calculations of the field structure are difficult, so in this paper we evaluate the field dependencies numerically in the framework of our model.) Such comparison is presented in Fig.2 for the time $t = t_0 \sim 190$ when the particle reaches the output side of the system. From Fig. 2 we observe that for dispersiveless and dispersive cases (left and right panels in Fig.2 respectively) the fields $E_x(x,t)$ have well-defined resonances in the wavenumber domain $E_x(k,t)$ at $k_s \simeq k_{s0} \simeq 4.33$ (resonance point). One can conclude that in this point a resonant interplay arises between the plasmonic-polariton spectrum and the modulating particle field. Corresponding changes are resonantly accumulated within the system length that finally leads to considerable modification of the

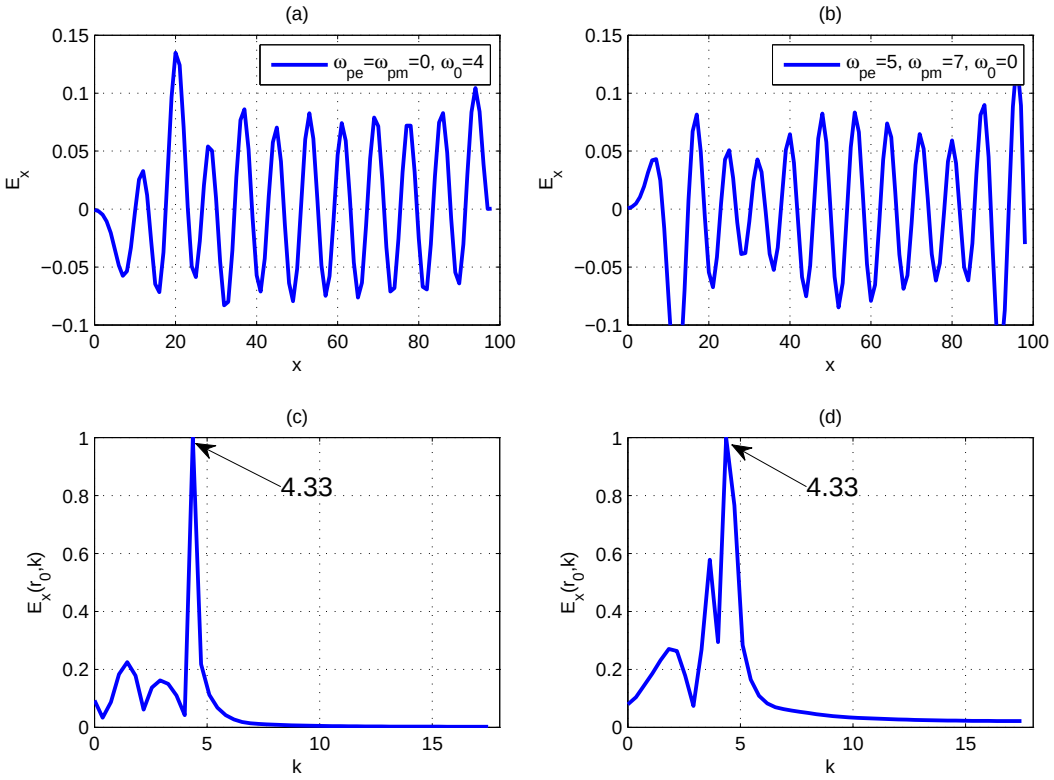

Figure 2: Field spatial structure $E_x(x,t_0)$ in dispersiveless (left panels) and dispersive materials (right panels) accordingly for the time $t = t_0 \simeq 190$ when the particle arrives the output of the system. (a) Field $E_x(x,t_0)$ for dispersiveless case and $\omega_0 = 4.0$; (b) spatial field in dispersive metamaterial but for $\omega_0 = 0$; (c) Fourier spectrum (wavenumber domain) $E_x(k,t_0)$ for (a) case; (d) Fourier spectrum $E_x(k,t_0)$ for (b) case. We observe well-defied peaks k_s in both cases with $k_s \simeq k_{s0} \simeq 4.33$. See details in text.

field shape along the particle path.

Now we turn to other cases of the velocity v_0 and modulation frequency ω_0. To understand the effect deeper it is important to investigate the Doppler shift of the frequency ω_0 with respect of the rest metamaterial. For dispersiveless case ($n = const$) the shifted frequency is calculated explicitly as $\omega_{s0} = \omega_0/(1 + v_0 n/c)$. However in dispersive case the shifted frequency ω_{s0} acquires dependence on the dispersive refraction index of medium $n(\omega)$. For this situation the shift already has to be evaluated from the complete equation $\omega_{s0} = \omega_0/(1 + v_0 n(\omega_{s0})/c)$. The latter already requires the formulation of the dispersive material model for $n(\omega)$. But in used FDTD approach (the time domain) such the shift should be formed by a self-consistent way in NIM model, where in some frequency ranges the negativity of $Re(n(\omega))$ can be reached. (In general the Doppler frequency shift has a nonlinear dependence on the modulating frequency, see details in Ref.[12].)

It is readily to see that k_s peak is calculated from the Doppler shift as $k_s = \omega_{s0} n/c =$

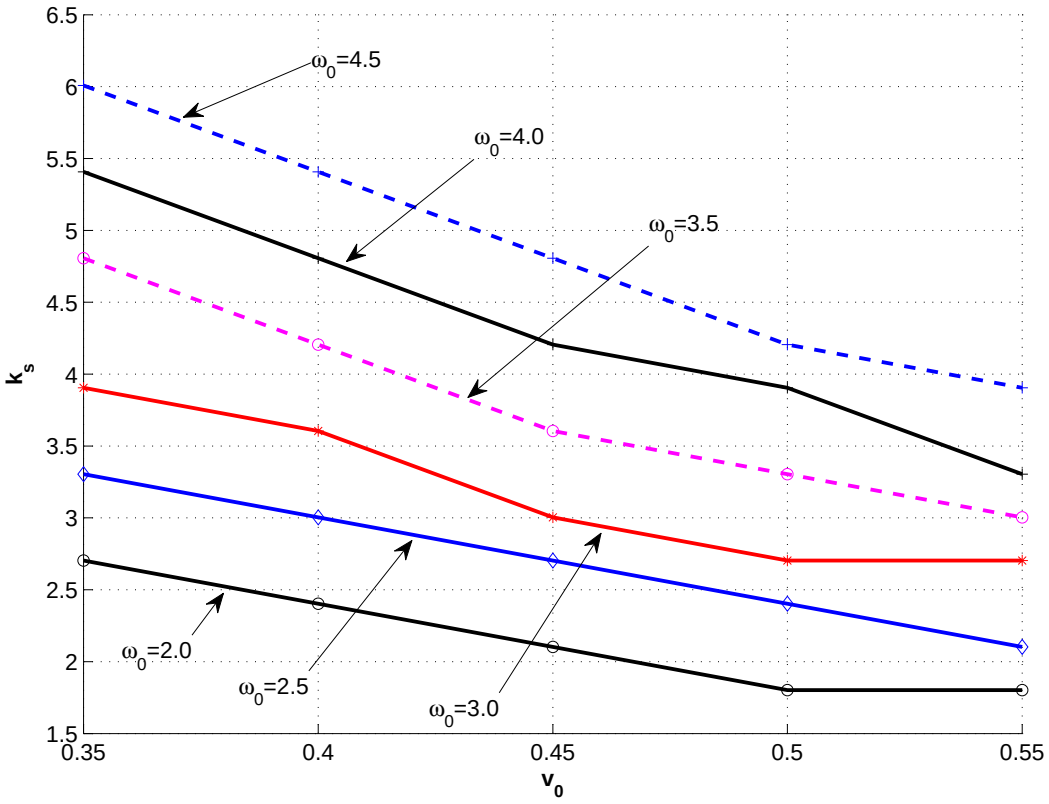

Figure 3: The dependence of the spectral peak position (wavenumber k_s) of the field $E_x(x,t)$ on the particle velocity v_0 for different ω_0 at $t \sim 190$ in dispersiveless case.

$\omega_0 n/c(1+v_0 n/c)$. To verify if the observed k_s is related to the Doppler shifted frequency ω_0 in Fig.3 the dependence $k_s = k_s(v_0)$ for various frequencies ω_0 in the dispersiveless case is shown. From Fig.3 we observe that (in used normalization) the wavenumber peak is about $k_s \simeq 4.33$ for $\omega_0 \simeq 4, v_0 = 0.52$ that coincides with peak $k_{s0} = 4.33$ for no-modulated source at $v_0 = 0.52$ for NIM in Fig.1 (a). Thus, we conclude that for $\omega_0 \simeq 4$ and $v_0 \simeq 0.52$ a spatial resonance arises due to Doppler effect around of $|k_s - k_{s0}|$.

Finally we study the frequency spectra of the Cherenkov emission for different values of ω_0 and v_0. In the frequency domain the dispersive permittivity and permeability have the following form ([29] Chapter 9) $\varepsilon(\omega) = \varepsilon_h - \omega_{pe}^2/(\omega^2 + i\gamma_e\omega)$ and $\mu(\omega) = \mu_h - \omega_{pm}^2/(\omega^2 + i\gamma_m\omega)$. For such $\varepsilon(\omega)$ and $\mu(\omega)$ the complex refraction index for the NIM metamaterial can be written as [32]

$$n(\omega) = \sqrt{|\varepsilon(\omega)\mu(\omega)|}\, e^{i[\phi_\varepsilon(\omega)+\phi_\mu(\omega)]/2}. \tag{4}$$

In this case a peak frequency $\omega = \omega_C$ has to be substituted into $\varepsilon(\omega), \mu(\omega)$ and then

in $n(\omega)$ Eq.(4). Fig. 4 (left and right panels respectively) show the structure of field $E_x(\mathbf{r}, t)$ and the complex refractive indices $n(\omega)$ in NIM for the cases different particle modulating frequencies ω_0 and velocity $v_0 = 0.52$. We observe from Fig. 4 (a) that the field structures corresponds to the inverse Cherenkov emission. Fig. 4 (c) shows that for $\omega_0 = 2$ the plasmon-polaritons excitation (PPE) are generated at the peak frequency $\omega_C = 3.77$ where the complex refractive index is $n(\omega_C) = -0.87 - i8.10 \cdot 10^{-5}$. For larger frequency $\omega_0 = 3.9$ the field E_x has monotonic spatial structure, see Fig. 4 (b) that allows exciting PPE at the peak frequency $\omega_C = 3.83$ where $n(\omega_C) = -0.77 - i8.09 \cdot 10^{-5}$. In both cases $Re(n) < 0$, thus, the optical waves have negative phase velocity that corresponds to reverse Cherenkov emission in NIM.

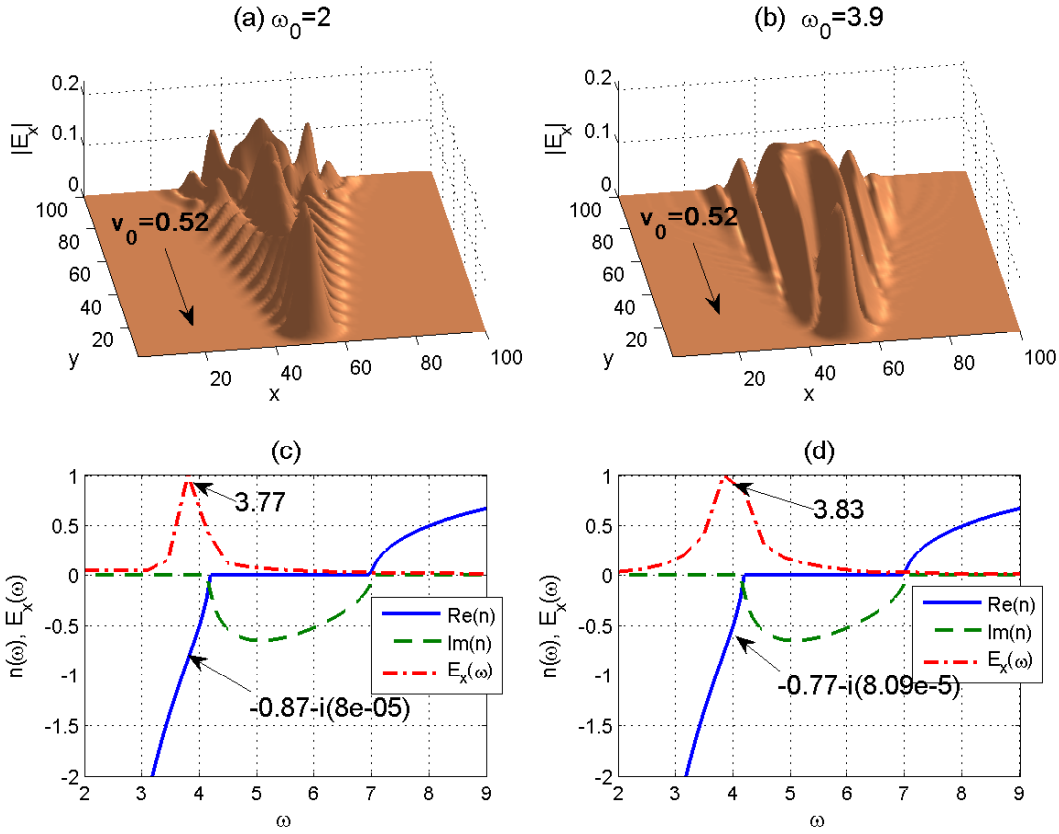

Figure 4: Snapshots of fields $E_x(\mathbf{r}, t)$ and the complex refractive indices $n(\omega)$ in NIM for velocity $v_0 = 0.52$ and different modulated frequencies ω_0. (a) Field E_x for $\omega_0 = 2$ corresponds to the plasmonic-polariton excitation (PPE) at the peak frequency $\omega_C = 3.77$ where $Re(n(\omega_C)) = -0.87$ indicated in (c); (b) field E_x for $\omega_0 = 3.9$ that generate PPE at the peak frequency $\omega_C = 3.83$ where $Re(n) = -0.77$.

The situation for smaller v_0 is shown in Fig. 5. Fig. 5 (left and right panels respectively) show the structure of field $E_x(\mathbf{r}, t)$ and the complex refractive indices $n(\omega)$ in NIM for the

cases of particle with different modulating frequencies ω_0 and particle velocity $v_0 = 0.35$. We observe from Fig. 5 (c) that for $\omega_0 = 2$ the plasmon-polaritons excitation (PPE) are generated at the peak frequency $\omega_C = 3.76$ where the complex refractive index is $n = -0.89 - i0.81 \cdot 10^{-5}$.

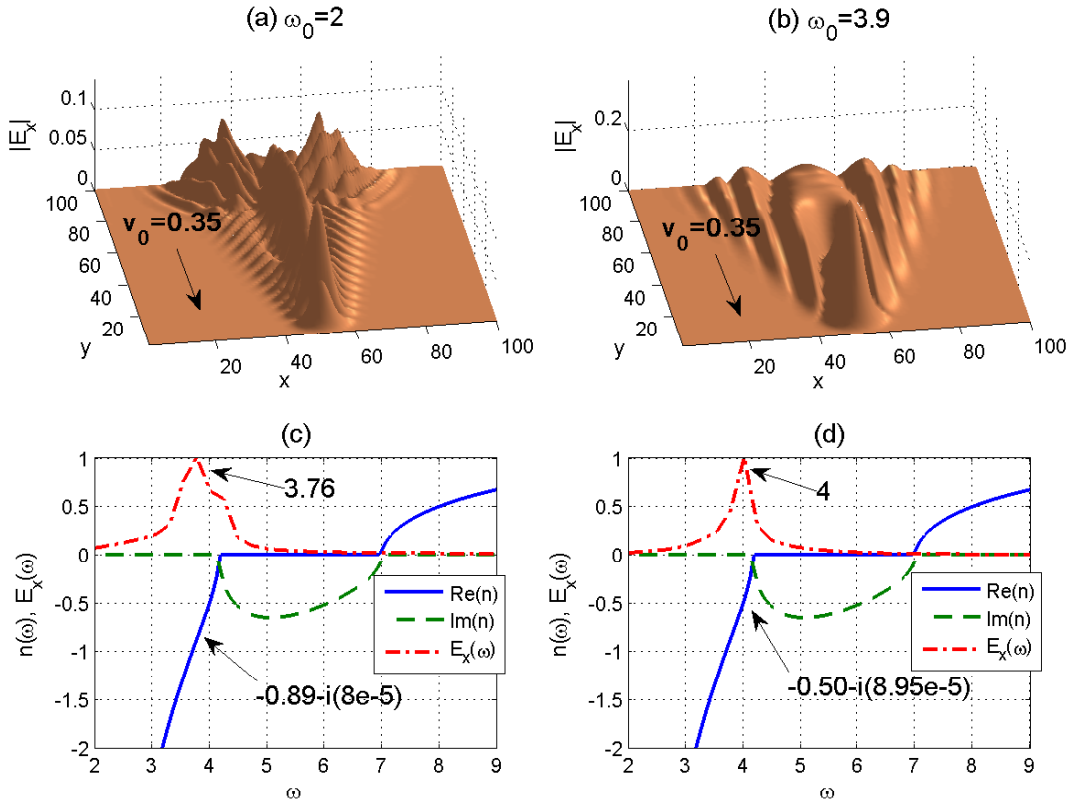

Figure 5: The same as in Fig. 4 but for velocity $v_0 = 0.35$. (a) Field E_x for $\omega_0 = 2$ that generates the plasmon-polaritons excitation (PPE) at the peak frequency $\omega_C = 3.76$ where $Re(n) = -0.89$ (c); (b) field E_x for $\omega_0 = 3.9$ that generate PPE at the peak frequency $\omega_C = 4$ where $Re(n) = -0.50$.

Fig.4 and Fig.5 show that the considered spatial resonance between the modulating frequency ω_0 and the plasmonic-polariton excitations: (i) happens in the frequency range where $Re(n)$ is negative and the inverse Cherenkov emission occurs, and (ii) the value of the metamaterial refraction index (and thus the polariton phase velocity) depends on the particle velocity v_0. The latter in principle allows to control the property of PPE in metamaterial.

3 Photonic crystals

In our simulations, we consider a photonic crystal slab [33, 34] fulfilled by periodical rods that is shown in Fig. 6.

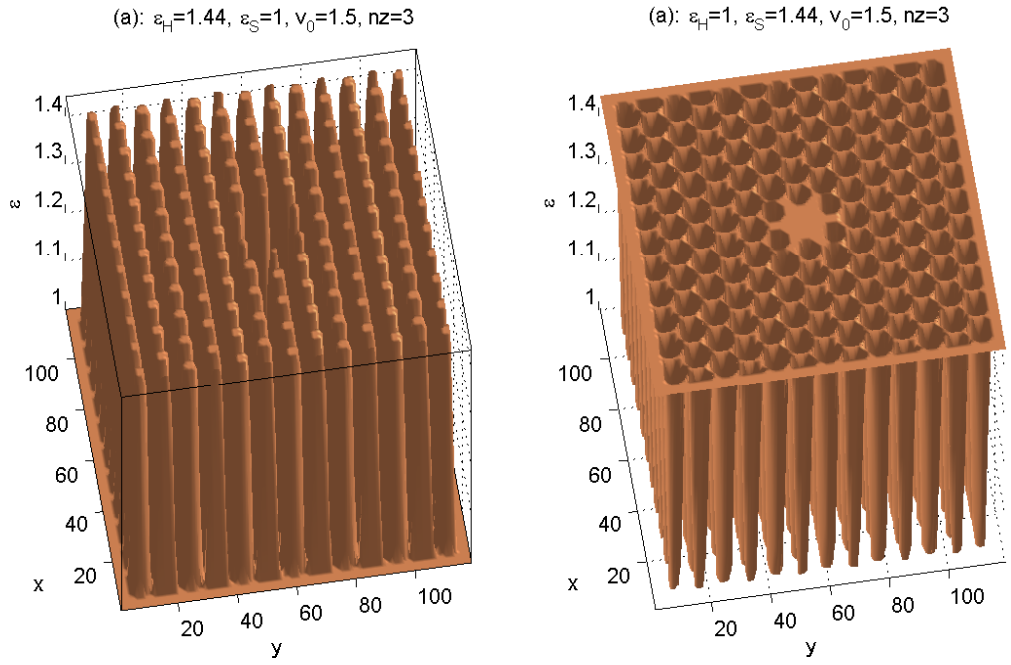

Figure 6: (Color on line) The average dielectric permittivity $\varepsilon(x, y)$ of a typical 2D photonic structures composed by a slab with dielectric permittivity ε_S and dielectric rods with dielectric permittivity ε_H: (a) dielectric rods (cylinders) placed in air, $\varepsilon_S = 1$, and (b) air holes with $\varepsilon_H = 1$ perforating a dielectric slab with ε_S. The periodical structure can have a defect placed in the central part of the system.

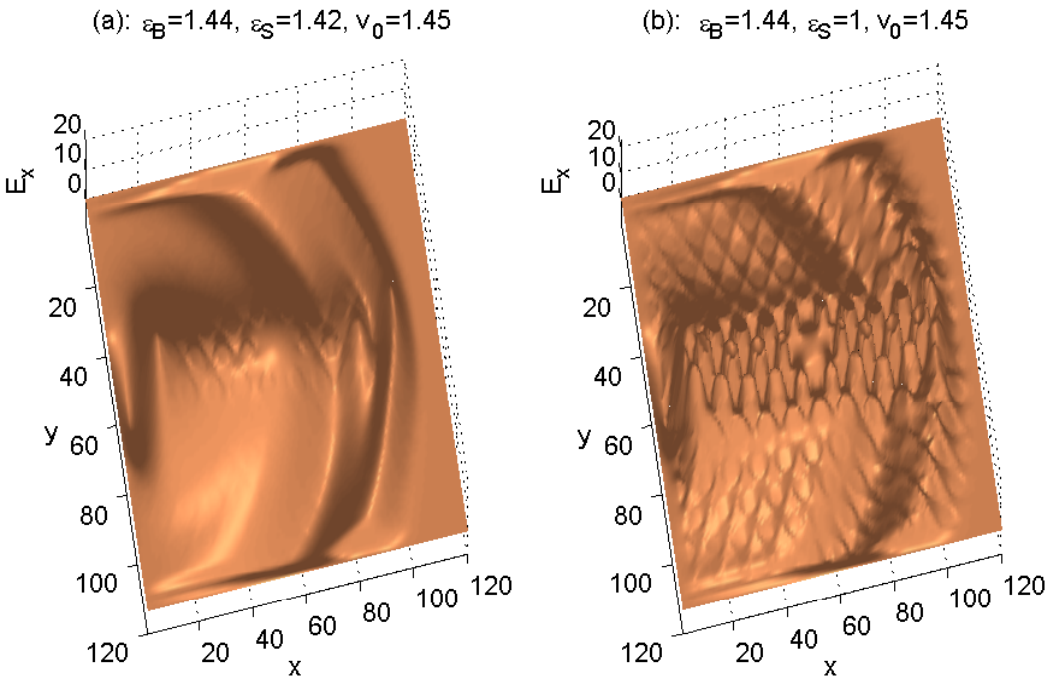

Figure 7: (Color online) Spatial structure of the electric field E_x generated by a source with velocity $v_0 = 1.45$. (a) Snapshot of Cherenkov cone radiation in a homogeneous medium with $\epsilon_C = \epsilon_S = 1.44$. (b) Snapshot of Cherenkov cone radiation in a real photonic crystal with $\epsilon_H = 1.44$, and $\epsilon_S = 1$. We observe the strong field oscillations generated within the Cherenkov cone.

Since the refractive index of photonic system variates in space and it is defined only locally (or in average), the Cherenkov emission in such 3D inhomogeneous photonic systems can be calculated only numerically. To realize our FDTD simulation we use the approach from Ref. [34] that we have elaborated for our purposes. In such 3D system the "numerical" velocity of light is $c = \sqrt{3}$. In Fig. 7 the cylinders radius and the slab thickness are chosen to be $r = 0.35a$ and $h = 0.50a$, respectively, where a represents the lattice constant of the photonic crystals. First, for references purposes we fix the particle velocity v_0 and consider the nearly homogeneous photonic crystal with the dielectric permittivities ε_H and ε_S such that the difference $\Delta\varepsilon = |\varepsilon_H - \varepsilon_S|$ is small, 7 (a).

Second, to see how the difference $\Delta\varepsilon$ affects the emission field structure we study the case of real PhCr when $\Delta\varepsilon$ is not small 7 (b). Such simulation for the electric field component E_x for the particle velocity $v_0 = 1.45 > v_c = c/\eta$ is shown in Fig. 7 (a) and Fig. 7 (b) respectively. We observe that the field shape displayed in Fig. 7 (a) has a structures typical for Cherenkov emission in homogeneous meduim with well-defined cone of radiation with small-valued field into such cone. However Fig. 7 (b) shows that the spatial structure E_x in real PhC changes considerably with respect of homogeneous case: the field inside of the Cherenkov cone is fullfilled by the oscillating

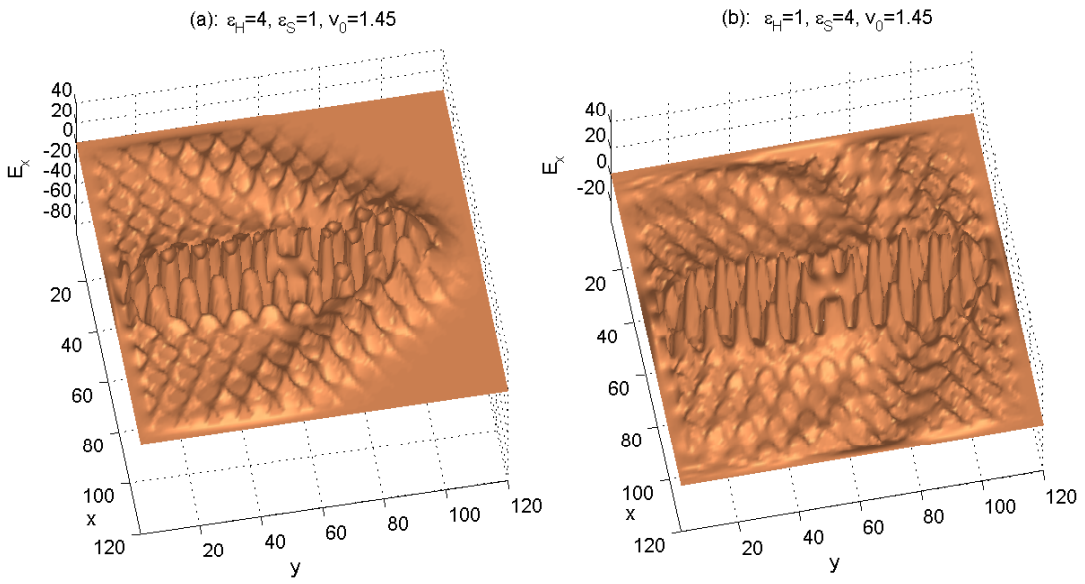

Figure 8: (Color online) Snapshots of the electric field E_x in a photonic crystal for $v_0 = 1.45$. (a) The peaks of the field oscillations coincide with the position of the cylindrical defects in the PhC slab structure, when $\epsilon_H = 4 > \epsilon_S = 1$. (b) The electromagnetic peaks is located beyond the dielectric rods if $\epsilon_H = 1 < \epsilon_S = 4$.

peaks corrsponding to the periodical rods. We found that the Cherenkov cone angle in Ph.C can be approximatelly defined as $\cos\theta = c/v_0\overline{\eta}$, where $\overline{\eta} = \sqrt{\overline{\varepsilon}}$, $\overline{\varepsilon}$ is the average dielectric permittivity of the system.

4 CONCLUSIONS

- We numerically studied the Cherenkov optical emission by a nonrelativistic modulated source crossing 3D dispersive metamaterial.
- It is found that the resonant interaction of the field produced by the modulated source with the spectrum of the periodic plasmonic-polariton excitations leads to considerable change of spatial structure for the Cherenkov emission.
- The field acquires monotonic shape in the frequency range where the dispersive refractive index of metamaterial is negative and the reversed Cherenkov radiation is generated.
- This effect opens new interesting possibilities in various applications metamaterials and photonic crystals in nanophotonics with the potential for creating and control light confining structures to considerably enhance light-matter interactions.

REFERENCES

[1] V.G. Veselago. The electrodynamics of substances with simultaneously negative values of ε and μ, *Sov. Phys. Usp.*, Vol. **10**, 509, (1968). [Usp.Fiz.Nauk 92, 517 (1967)].

[2] V.M. Shalaev, Optical negative-index metamaterials, *Nature Photonics*, Vol. **1**, pp. 41–48, (2007).

[3] C.M. Soukoulis, M. Wegener, Past achievements and future challenges in the development of three-dimensional photonic metamaterials, *Nature Photonics*, Vol. **5**, pp. 523–530, (2011).

[4] O. Hess, J. B. Pendry, S. A. Maier, R. F. Oulton, J. M. Hamm, K. L. Tsakmakidis, Active nanoplasmonic metamaterials, *Nature Materials*, Vol. **11**, pp. 573–584, (2012).

[5] Huanyang Chen, C. T. Chan , Ping Sheng, Transformation optics and metamaterials, *Nature Materials*, Vol. **9**, pp. 387–396, (2010).

[6] J.A. Gordon, R. W. Ziolkowski, CNP optical metamaterials, *Opt. Express*, Vol. **16**, pp. 6692-6716, (2008).

[7] G.W. Milton, Realizability of metamaterials with prescribed electric permittivity and magnetic permeability tensors, *New Journal of Physics*, Vol. **12**, 033035, (2010).

[8] V. Podolskiy, A. Sarychev, V. Shalaev, Plasmon modes and negative refraction in metal nanowire composites, *Optics Express*, Vol. **11**, 7, pp. 735-745, (2003).

[9] V. M. Shalaev, Wenshan Cai, Uday K. Chettiar, Hsiao-Kuan Yuan, A. K. Sarychev, V. P. Drachev, A. V. Kildishev, Negative index of refraction in optical metamaterials, *Opt. Lett.*, Vol. **30**, 24, pp. 3356-3358, (2005).

[10] G. Burlak, A. D-de-Anda, R. Santaolaya Salgado, J. Perez Ortega, Narrow transmittance peaks in a multilayered microsphere with a quasiperiodic left-handed stack, *Optics Commun.*, Vol. **283**, 19, pp. 3569–3577, (2010).

[11] G. Burlak, Spectrum of Cherenkov radiation in dispersive metamaterials with negative refraction index, *Progress In Electromagnetics Research,* Vol. **132**, pp. 149-158, (2012).

[12] G. Burlak , V. Rabinovich, Time-Frequency Integrals and the Stationary Phase Method in Problems of Waves Propagation from Moving Sources, *Symmetry, Integrability and Geometry: Methods and Applications*, Vol. **8**, 096, 21, (2012).

[13] G.Burlak, A. D-de-Anda, The field confinement, narrow transmission resonances and Green function of a multilayered microsphere with metamaterial defects, *Journal of Atomic, Molecular, and Optical Physics*, Vol. Article ID 217020, pp. 1–13, (2011).

[14] Shumin Xiao, V. P. Drachev, A. V. Kildishev, Xingjie Ni, Uday K. Chettiar, Hsiao-Kuan Yuan, V. M. Shalaev, Loss-free and active optical negative-index metamaterials, *Nature*, Vol. **466**, pp. 735–738, (2010).

[15] Subimal Deb, S. Dutta Gupta, Absorption and dispersion in metamaterials: Feasibility of device applications, *J. Phys.*, Vol. **75**, 5, (2010).

[16] P.A. Cherenkov, Visible emission of clean liquids by action of γ-radiation, *Dokl. Akad. Nauk.*, Vol. **2**, pp. 451–454, (1934).

[17] Yu. O. Averkov, V. M. Yakovenko, Cherenkov radiation by an electron particle that moves in a vacuum above a left-handed material *Phys. Rev. B*, Vol. **79**, pp. 193402–193412, (2005).

[18] Z. Y. Duan, B.I. Wu, S. Xi, H. S. Chen, M. Chen, Research progress in reversed cherenkov radiation in double-negative metamaterials, *Progress In Electromagnetics Research*, Vol. **90**, pp. 75–87, (2009).

[19] Sheng Xi, Hongsheng Chen, Tao Jiang, Lixin Ran, Jiangtao Huangfu, Bae-Ian Wu, Jin Au Kong, Min Chen, Experimental Verification of Reversed Cherenkov Radiation in Left-Handed Metamaterial, *Phys. Rev. Lett.*, Vol. **103**, 194801, (2009).

[20] Yu.O. Averkov, A. V. Kats, and V. M. Yakovenko, Electron beam excitation of left-handed surface electromagnetic waves at artificial interfaces *Phys. Rev. B*, Vol. **72**, pp. 205110–205114, (2005).

[21] Jun Zhou, Zhaoyun Duan, Yaxin Zhang, Min Hu, Weihao Liu, Ping Zhang, Shenggang Liu, Numerical investigation of Cherenkov radiations emitted by an electron beam particle in isotropic double-negative metamaterials, *Nuclear Instruments and Methods in Physics Research Section A*, Vol. **654**, 1, pp. 475–480, (2011).

[22] Z. Y. Duan , Y. S. Wang, X. T. Mao, W. X. Wang, and M. Chen, Experimental demonstration of double-negative metamaterials partially filled in a circular waveguide, *Progress In Electromagnetics Research,* Vol. **121**, pp. 215–224, (2011).

[23] Zhu, Lei, Fan-Yi Meng, Fang Zhang, Jiahui Fu, Qun Wu, Xu Min Ding, and Joshua Le-Wei Li. An Ultra-Low Loss Split Ring Resonator by Suppressing the Electric Dipole Moment Approach. *Progress In Electromagnetics Research* Vol. **137**, pp. 239-254, (2013).

[24] Zhaoyun Duan, Chen Guo, Min Chen, Enhanced reversed Cherenkov radiation in a waveguide with double-negative metamaterials, *Opt.Express*, Vol. **19**, pp. 13825–13830, (2011).

[25] Ginzburg V L Radiation by uniformly moving sources (Vavilov-Cherenkov effect, transition radiation, and other phenomena) *Phys. Usp.* Vol. **39**, pp. 973–982, (1996).

[26] J.D. Jackson, *Classical electrodynamics*, John Willey and Sons, (1975).

[27] K.E. Oughstun, *Electromagnetic and Optical Pulse Propagation 2: Temporal Pulse Dynamics in Dispersive*, Attenuative Media (Springer Series in Optical Sciences), Springer, (2009).

[28] Yeh, P., *Optical waves in Layered Media* , John Wiley and Sons, New York, 1988.

[29] A. Taflove, S. C. Hagness, *Computational Electrodynamics: The Finite-Difference Time-Domain Method*, Artech House, Boston, (2005).

[30] J. Schneider, *Understanding the Finite-Difference Time-Domain Method*, www.eecs.wsu.edu/∼schneidj/ufdtd, (2010).

[31] G.N. Afanasiev, *Cherenkov Radiation in a Dispersive Medium, Vavilov-Cherenkov and Synchrotron Radiation, Fundamental Theories of Physics*, Kluwer Academic Publishers, (2004).

[32] R.W. Ziolkowski, Superluminal transmission of information through an electromagnetic metamaterial, *Phys. Rev. E*, Vol. **63**, 046604, (2001).

[33] J.D Joannopoulous, R. D. Meade, and J. N Winn, Photonic crystal: modeling the flow of light, Princenton University Press., Princeton, NJ, 1995.

[34] Se-Heon Kim, Sun-Kyung Kim, and Yong-Hee Lee, Vertical beaming of wavelength-scale photonic crystal resonators, Physical Review, B 73, 235117 (2006).